
Libraries of hidden layer activity patterns can lead to better understanding of operating principles of deep neural networks

Jung Hoon Lee
 Allen Institute for Brain Science
 Seattle, WA 98109
 jungl@alleninstitute.org

Abstract

Deep neural networks (DNNs) can outperform human brains in specific tasks, but due to their lack of transparency in decision-making processes, it remains uncertain whether we can completely rely on DNNs when it comes to high-risk problems requiring rigorous decisions. As DNNs' operations rely on a massive number of linear/nonlinear computations in both parallel and sequential, it is impossible to distinguish every factor influencing their decision. Further, DNNs cannot be empirically tested in every potential condition. Therefore, we should consider the possibility that DNNs' decisions can be corrupted by unexpected factors; for instance, adversarial attacks can deceive DNNs quite effectively. Before DNNs are deployed to solve high-stakes problems, such vulnerability must be overcome. In our study, we propose an algorithm to provide better insights into DNNs' decision-making processes. Our experiments suggest that this algorithm can effectively trace DNNs' decision processes on a layer-by-layer basis and be used to detect adversarial attacks.

1 Introduction

There is no doubt that remarkable successes [9] in deep learning (DL) has led us to believe that agents trained by DL, deep neural networks (DNNs) could replace humans in difficult and/or sometimes life threatening situations. However, DNNs depend on a huge number of both linear and nonlinear operations, making their decisions incomprehensible to us [16, 13, 6, 1], and we often refer to DNNs as black box systems due to this inexplicability. We have seen the effectiveness of DNNs in a very complicated board game 'Go' against Sedol Lee, but the reasons behind AlphaGo's decisions remain in the dark and baffled many professional human Go players.

Adopting the current DNNs/DL in some tasks may be acceptable, but blindly trusting DNNs' decisions may be perilous in high-stakes decisions [22]. For instance, we could build a cancer diagnosis system to help patients or future patients, but a reliable diagnosis must reveal underlying factors, with which its precision can be evaluated. However, current DNNs cannot explain their decisions, and this lack of transparency should not be ignored. In principle, we need an estimator to approximate DNNs' operations to fully understand their decision-making processes, but given the complexity of DNNs, building a reliable estimator is extremely challenging.

To gain insights into DNNs' operating principles, a line of studies analyzed properties of hidden neurons which represent intermediate stages of DNNs' decisions. First, feature visu-

alization was proposed to gain insight into response characteristics of hidden neurons [18, 3]. Specifically, this approach allows users to identify optimal visual features that can stimulate target hidden neurons. With such optimal visual features, we can better understand how DNNs are trained; see also [5, 23]. Second, the features of hidden layers were studied to better understand DNNs’ operations [2, 17, 14]. Layer-specific features were analyzed with clustering algorithms and linear classifier. For instance, Allain and Bengio [2] tested linear-separability of the features in hidden layers and found that linear separability increases monotonically, as the selected layer is closer to the last layer. Third, a set of single neurons’ responses evoked by multiple examples were used as feature vectors, which are different from those evoked by the same input. Raghu et al. [21] used them to study how well the hidden layers were correlated with ground truth (i.e., the labels of inputs).

In line with these earlier studies, we sought an algorithm that can explain DNNs’ answers from hidden layer activity patterns (HAPs). By ‘explain’, we mean that the algorithm should allow us to predict DNNs’ answers/decisions from HAPs on unseen examples (i.e., test examples); it should be noted that we aim to predict DNN’s answers/decisions rather than the true labels of input patterns. To this end, we assumed 1) that HAPs’ meanings are all relative, and their meanings become apparent only when they are compared with one another and 2) that HAPs evoked by the same-class inputs are clustered together; importantly, the number of HAPs clusters does not have to be equal to the number of classes. That is, we need effective methods to estimate similarities among HAPs. In doing so, we turn to our earlier short-term memory systems [11] that can calculate cosine similarities between present input patterns and stored patterns. They also store input patterns using synaptic weights, when an input pattern is substantially different (i.e., novel) from the stored patterns. Our empirical evaluations showed that the short-term memory systems can catalog HAPs and be used to predict DNNs’ answers on test examples. We further found that the short-term memory systems can effectively detect the presence of adversarial attacks.

2 Network structures and operations

Our short-term memory system [11] stores novel input patterns (i.e., substantially different from stored input patterns), and its outputs reflect cosine similarities between a present input and stored inputs. If HAPs, evoked by the same class input patterns, are well clustered together, the stored input patterns in the memory systems can approximate distributions of input patterns (i.e., HAPs). That is, the stored HAPs can serve as reference points for HAPs’ clusters. With this possibility in mind, we use the short-term memory systems, which will be referred to as ‘library networks’ hereafter, to inspect the diversity of HAPs and study their links to DNNs’ decisions.

2.1 Generating libraries of activity patterns in hidden layers

As shown in Fig. 1, a library network has a single synaptic weight layer and accepts normalized HAPs (Eq. 1) as inputs.

$$h_i^k = \sum_j w_{ij} \frac{f_j^k}{\|\vec{f}_k\|^2}, \text{ where } w_{mn} = \frac{f_n^m}{\|\vec{f}_m\|^2} \quad (1)$$

, where h_i^k represents a synaptic input to output node i of library networks evoked by the input pattern k .

It performs two tasks mainly [12]. First, it estimates activations for inputs and finds maximal activations. When maximal activations are below the predefined threshold value (θ), the inputs are labeled as novel. Second, it stores novel inputs by adding output nodes and imprinting inputs to synaptic weights targeting newly added nodes (Eq. 1); that is, a newly added node effectively ‘stores’ a present input pattern. As output neurons are continuously added, its size is determined by characteristics of HAPs and the threshold value; naturally, the higher the chosen threshold value is, the bigger the constructed library networks are.

In the experiments, we construct library networks for multiple hidden layers while introducing all training examples. Once the library networks are fully constructed with training

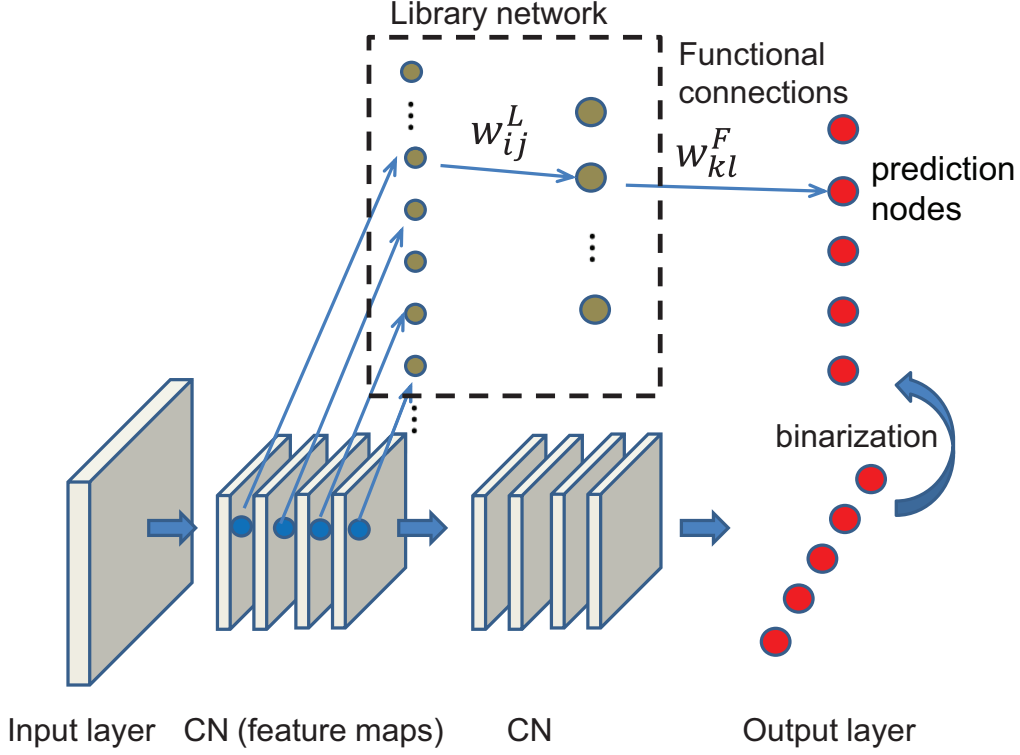


Figure 1: The structure of library networks. The schematics of a library network are shown in the top row of the figure, whereas the bottom line shows a DNN consisting of multiple convolutional layers (CLs) and a fully-connected (FC) layer, which is chosen for illustration. For clarification, a single library network is displayed. CN layers produce multiple sheets of feature maps, and all nodes within them are mapped onto input nodes of the library network (clarified in a dashed box). Similarly, all outputs of FC layers are introduced to the library networks. The output nodes of the library networks are determined by the properties of input patterns (outputs of hidden neurons). Then, the outputs of library networks are correlated with prediction nodes derived from DNNs’ answers via binarization. In the experiments, we also construct the library networks for blocks of layers used in ResNet. The outputs of these blocks are modulated with batch normalization before introduction to the library networks.

examples, they can estimate cosine similarities between a present HAP and stored ones. If a previously stored HAP is presented again to a library network, the activation of output node, added when it was presented, will be 1, but all other activations are smaller than 1.

2.2 Functional connections between library networks and decisions

The motivation of using library networks can be easily explained with an extreme case, in which HAPs clusters are well separated. Suppose that HAPs in the same cluster are extremely similar to each other but significantly different from those in different clusters. Naturally we can assume 1) that the size of library network (i.e., the number of output nodes) is the same as the number of HAPs’ clusters and 2) each output node stores a single example from each cluster. With these well separated HAPs’ clusters, activating the output nodes can clearly determine to which cluster the present HAP belongs. In DNNs, such an extreme case may not hold, but we assume that training can force HAPs to cluster together depending on input patterns and that library networks can still predict DNNs’ answers. Conversely, we can use these (hypothetical) functional links between library networks and DNNs’ answers to evaluate how well the hidden layers are trained to find the correct answers.

To address this possibility of functional links and their utilities, DNNs' answers are first transformed into binary vectors and introduced into prediction nodes (Fig. 1), and we establish correlations between library networks' output nodes and prediction nodes using the Hebbian-rule (Eq. 2):

$$W_{mn}^F = \sum_k g(h_n^k) \times O_m^k, \text{ where } g(x) = \exp\left(\frac{-(1-x)}{0.01}\right) \quad (2)$$

, where W_{mn}^F denote the functional connections from library network node n to prediction node m . During the construction of these functional links, the inputs to prediction nodes corresponding to the DNNs' answers are 1, all other inputs are -1. It should be noted that output nodes of the library networks have nonlinear kernels (Eq. 2) to make their activations sparse, rendering sharper correlations. The training examples are used to establish the functional connections between library networks and DNNs' answers (Fig. 1). With these functional connections, we test the library networks' ability to predict DNNs' decisions on unseen (training) examples by estimating the forward inputs to prediction nodes and using three or eight maximally activated output nodes of library networks (Eq. 3)

$$P_m^k = \sum_{a=1}^{a=3,8} W_{ma}^F \times \text{sort}(h^k)_a \quad (3)$$

, where $\text{sort}(h^k)_a = (h_{\text{argmax}(h^k)[0]}^k, h_{\text{argmax}(h^k)[1]}^k, \dots)$; $\text{argmax}(V)$ represents indices of vector V components sorted in descending order.

3 Results

3.1 Empirical evaluations of utilities of library networks

In this study, we test the utilities of library networks using two DNNs, 1) a convolutional network (CNN) trained with MNIST dataset [10] and 2) a ResNet trained with CIFAR10 dataset [8]. MNIST includes 60,000 training examples and 10,000 test images of handwritten digits (0–9). Each image consists of 28-by-28 8-bit gray pixels. CIFAR-10 is the collection of 10 classes of items ranging from animals to man-made devices. Each class has 500 training and 100 test examples, each of which is a 32-by-32 color image.

Both CNN and ResNet are implemented using 'Pytorch', the open-source python machine learning libraries [19]. CNN used here is an implementation of a variation of LeNet-5 [10] consisting of 2 convolutional (CN) layers and 2 fully-connected (FC) layers. We adopted the official implementation of 'pytorch' [20] and trained it with default parameters in the official example. For ResNet, we adopt pre-trained networks and implementation of ResNet44 available in the public github repository [7]; ResNet44 will be referred to as ResNet. Using these datasets and networks, we test the predictive power of the library networks constructed for CNN and ResNet. All codes used in this study are freely available in the public github repository [12] without restriction.

3.2 Studying CNN through library networks

As the size of the library networks reflects the homogeneity of HAPs, we first measure the sizes of 4 library networks for CN1, CN2, FC1 and FC2 layers in the CNN, depending on threshold values (θ). When the same threshold value is used, the library networks of the earlier hidden layers are bigger than those of the later layers (Fig. 2A); for instance, the library network for FC1 is bigger than the others when the threshold value is chosen for all layers). That is, HAPs in the earlier layers are more heterogeneous, suggesting that the input vectors are transformed into homogenous ones (possibly, homogenous clusters), as information propagates through CNN.

Next, using the Hebbian rule (Eq. 2), we build functional connections (i.e., correlations) between 4 library networks and CNN's answers. Once the functional connections are established, we test how well the library networks can predict DNNs' answers/decisions (Eq. 3

and Section 2.2). Fig. 2B shows the prediction accuracies from all 4 library networks for CN1, CN2, FC1 and FC2 depending on θ . As shown in the figure, the library networks can reliably predict CNN’s answers on test examples, especially when the higher threshold values are chosen. We further test the predictive power of library networks by allowing them to provide three best answers. If CNN’s decision coincides with one of the three best answers proposed by the library networks, we count it as a correct answer. As shown in Fig. 2C, the library networks exhibit dramatically enhanced predictive power.

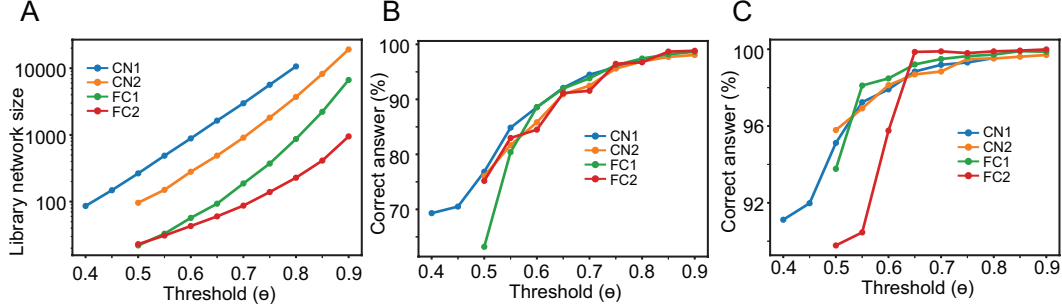


Figure 2: Empirical evaluations using the CNN trained for MNIST. (A), The sizes of library networks (i.e., the number of output nodes) depending on threshold values for novelty detection (see the text). The color codes are used to specify target layers. For instance, CN1 represents a library network’s size using HAPs from the first CN layer. (B), The fraction of correct predictions of the library networks using single best answers. (C), The same as (B) but the three best answers are used for predictions.

We note that the predictive power of the library networks for later layers are higher than those for the earlier layers when high θ is selected. This is consistent with the notion that input vectors are transformed progressively to networks’ decisions through layers (see Alain and Bengio [2], for instance). As the library networks appear to represent information regarding CNN’s decisions, we further track the changes in predictions from one layer to another by establishing the confusion index (CI) between two digits using each library network’s predictions. $CI(d_1, d_2)$ is the summation of the activations’ products corresponding to two digits, d_1 and d_2 (Eq. 4).

$$CI(d_1, d_2) = \frac{CA(d_1, d_2)}{CA(d_1, d_1)}, \text{ where } CA(d_1, d_2) = \sum_k \frac{\exp(P_{d_1}^k) \times \exp(P_{d_2}^k)}{\sum_{i=1}^{i=10} P_i^k} \quad (4)$$

We use trials (i.e., forward passes) to estimate CI , in which the best answers of the library networks correctly predict (i.e., recognize) the digits (denoted by d_1) presented to CNN. As such, CI can estimate the probability of the library networks’ misidentifying the input belonging to d_1 as d_2 on average. As $CI(d_1, d_1)$ is always 1, we do not report them below.

Figure 3 A-C shows the confusion matrices whose components are CI s, when $\theta = 0.65$. We do not display CI for FC2 because they are extremely low. The row represents d_1 (correct answer), and the column, d_2 , respectively. As shown in the figure, digit 9 confuses CN1 layer (i.e., the first CN). Interestingly, CN2 also shows relatively high CI values when digit 9 is presented (i.e., $d_1 = 9$). These confusions are alleviated in FC1 layer. To examine if this trend is a consequence of low θ , we increased $\theta = 0.75$ and found the equivalent results (Fig. 3 D-F). The high CI values in response to digit 9 ($d_1 = 9$) can be explained by that digit 9 has multiple visual features similar to those in other digits. Thus, CN layers, which rely on limited spatial filter, may have difficulty in differentiating 9 from others. FC layers, fully connected to previous layers, can use global features (e.g., locations of features) to precisely recognize digits. We also note that $CI(4, 9)$ is high in all layers. The prominent features of ‘4’ and ‘9’ look a like, and even these features are in similar locations. These suggest that CN layers are optimized to identify local features, while FC layers are optimized to utilize the (relative) locations of features detected by CN layers. Thus, we propose that the library

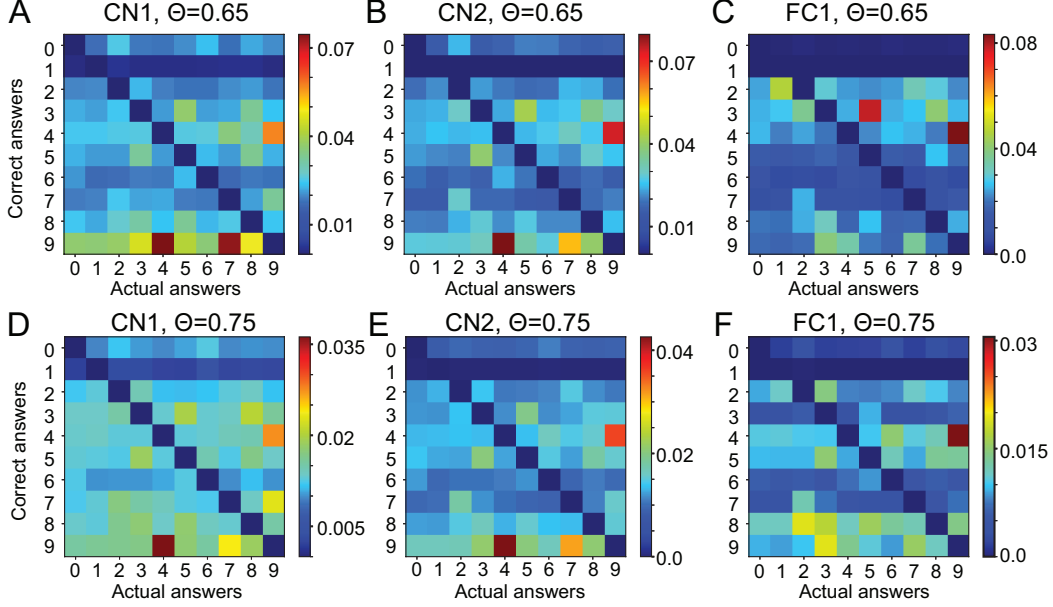


Figure 3: Confusion matrix. (A)-(C), The confusion indices estimated using library networks’ predictions constructed for CN1, CN2, FC1, respectively. Each row represents a confusion index for the correct digit. For instance, the values shown in the 10th row and 5th column represent the probability of library networks’ reporting digit ‘4’ in response to digit ‘9’. (D)-(F), The same as (A)-(C), but the threshold value is 0.75 instead of 0.65.

networks and confusion matrices help us infer workflows of DNNs consisting of CN and FC layers.

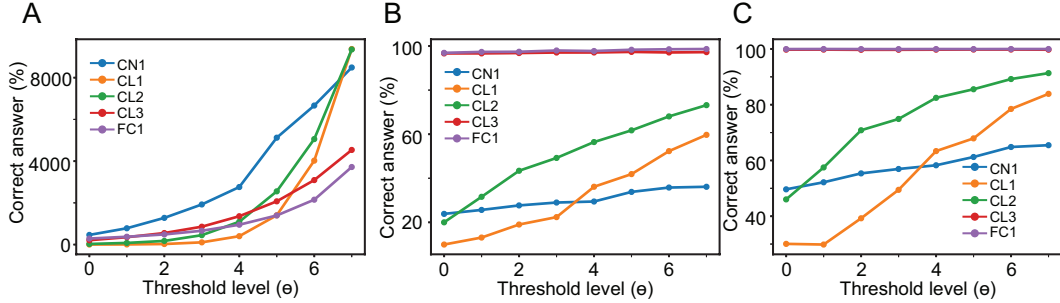


Figure 4: Empirical evaluations using the ResNet trained for CIFAR 10. (A), The sizes of library networks (i.e., the number of output nodes) depending on threshold levels for novelty detection. Since the homogeneity of HAPs varies significantly from one layer to another, a widely different set of threshold values is chosen for each layer. The actual values are listed in Table 1. (B), The fraction of correct predictions of library networks using single best answers. (C), The same as (B), but the three best answers are used for predictions.

3.3 Studying ResNet through library networks

We further test the library networks’ utilities via ResNet trained with CIFAR 10 dataset. Specifically, we use the pretrained ResNet44 network that was obtained from the github repository [7]. Although there are 44 layers in the ResNet, it is organized with 5 functional blocks. The three blocks, composite layers (CL) 1, 2 and 3, include multiple layers, and the

rest (CN1 and FC) include single layers. The library networks are constructed to inspect the 5 blocks instead of all hidden layers, and we repeat the same experiment. In the ResNet, we use 8 highest output activations of the library networks to predict their answers (Eq. 3).

We note that HAPs in the ResNet are heterogenous and that widely different θ are necessary to describe them properly. Specifically, we use 8 values of θ for CN1, CL1-3 and FC, respectively; see Table 1 for actual values. Figure 4 shows the accuracies of 5 library networks' predictions depending on the 8 values of θ . Although the accuracies are lower than those of MNIST case (Fig. 2), the library networks can still reliably predict the ResNet's decisions on test examples (Fig. 4B and C), which indicates that even HAPs in the ResNet are forced to cluster during training. We also note that HAPs in CL1 (e.g., the first composite layer) are more homogenous than those in any other blocks/layers in the ResNet (Fig. 4A), which is distinct from the gradual increase in HAPs' homogeneity in the CNN (Fig. 2A). This suggests that the main function of CL1 is to transform feature vectors of the CN1 into homogenous vectors and that the function of subsequent blocks/layers is to find optimal ways to map these highly homogenous vectors (from CL1) into proper clusters to reflect the classes of input patterns.

3.4 Adversarial attacks reduce consistency among library networks' predictions

The results above indicate that the library networks can predict DNNs' answers and that multiple library networks provide multiple predictions. In our experiments, we note that the library networks' predictions are largely consistent with each other and thus assume that consistency among predictions of library networks (CPL, hereafter) is the result of training DNNs; if DNNs are well trained, all parts of the networks are consistent with one another. This leads us to speculate that CPL could decrease when input vectors are drawn out of the trained-domain. We address this hypothesis by introducing adversarial inputs and measuring CPL using the correlations between prediction node outputs of library networks (Eq. 5).

$$\frac{1}{N} \sum_{i,j} \frac{\vec{P}_i^k \cdot \vec{P}_j^k}{\|\vec{P}_i^k\| \|\vec{P}_j^k\|}, \quad (5)$$

, where \vec{P}_i^k represents the vector of prediction outputs from i th library network in response to k th input patterns, and N is the number of possible pairs of layers. By the definition, we can get a single CPL value for an input pattern.

In our study, we use the routine 'LinfPGDAttack' included in the advtorch [4], which implements the projected gradient descent attack [15], to generate 200 adversarial images from MNIST and CIFAR 10 datasets, respectively. We fix the iteration number at 40 and step size at 0.01, while we test multiple perturbation sizes ϵ . CPLs are estimated according to Eq. 5 for 200 normal and adversarial images. To evaluate CPLs' dependence on the threshold value of each layer, we test 7 sets of threshold values (see Table 1). Fig. 5A shows the distributions of CPL calculated with set 1. As shown in the figure, CPLs are distinct and well separated between normal and adversarial images of MNIST dataset. To quantify how well they can be separated by an ideal observer, we calculated the area of the receiver operating characteristic curve (AUROC); see [24] for details. Fig. 5B shows the changes in AUROC depending on the degree of adversarial attacks (ϵ). The color codes represent the selected set of threshold values. We also test CPLs of ResNet between normal and adversarial inputs. As shown in Fig. 5C, the AUROC values can be higher than 0.8. Based on the results, we propose that CPL can be used to detect adversarial attacks or more broadly out-of-training examples.

4 Discussion

To probe DNNs' decision-making processes, we studied the functional links between HAPs and DNN's decisions using library networks. Our empirical evaluations show that the library networks can be used to predict DNNs' answers on test examples. This suggests 1) that HAPs are clustered during training and 2) that studying the functional clusters can shed

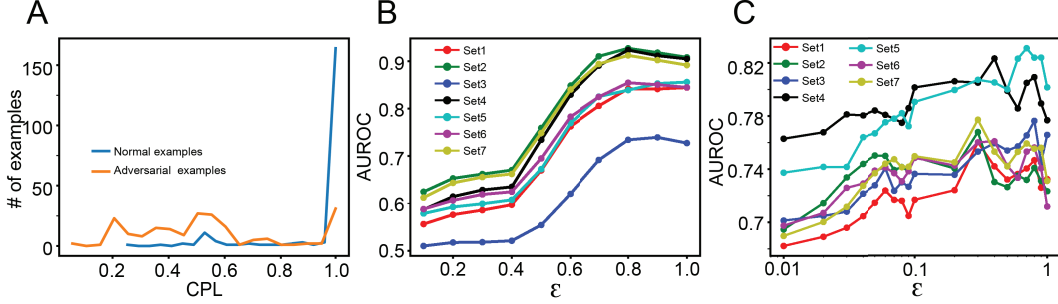


Figure 5: Detecting adversarial attacks: (A), The histogram of comparing CPL values between normal and adversarial examples. (B), AUROC calculated using CPL values from the CNN trained for MNIST, depending on the ϵ . The colors represent a set of threshold values chosen for the library networks; see Table 1 for the actual values. (C), The same as (B), but AUROC calculated from the ResNet.

light on DNNs’ internal processes. While in line with the earlier studies focusing on the properties of hidden neurons to explore DNNs’ operating principles, our study differs in that 1) it emphasizes the importance of similarities among HAPs in explaining DNNs’ decisions, 2) it proposes the library networks that can efficiently estimate similarities among HAPs to analyze DNNs’ decision-making processes and 3) it proposes potential links between CPL (consistency of predictions of library networks) and the adversarial attacks. Below we discuss the implications of our study in more detail.

4.1 Transparency of decision-making via a flowchart of decision-making

Library networks allow us to inspect how well the hidden layer activity is correlated with DNNs’ answers. While these correlations may not fully explain DNNs’ operations, they do allow us to look into their decision-making processes. As the confusion matrices can be used to infer functions of individual hidden layers, using it from the CNN experiments, we can speculate that 1) CN1 is trained to detect visual features necessary, 2) CN2 is trained to make the features more easily detectable, and 3) FC1 and 2 are trained to find ideal ways to utilize global features like features’ locations to make decisions. With the hidden layers’ potential functions, we can make an effective flowchart explaining DNNs’ decision processes.

Further, we note that it is possible to use the library networks to estimate the performance of individual layers and then selectively improve the underperforming layer. If the library networks suggest that the two classes cannot be clearly separated from each other in one of the CN layers (or a hypothetical functional block of DNNs assigned to feature-detection), we can conclude that more filters are needed for the CN layer (or blocks) and provide additional filters to improve the layer’s resolution power. We could train the added filters while keeping the old filters intact. Alternatively, if the library networks suggest that FC layers perform the desired tasks poorly, we can retrain FC layers with CN layers intact or add more FC layers to the networks to enhance DNNs’ performance.

4.2 Detecting out-of-training tasks/examples

DNNs can work properly only when the test inputs and training examples are drawn from the same domain. For instance, DNNs trained with MNIST dataset cannot properly recognize alphabet letters. However, even when DNNs receive the inputs drawn from other domains, DNNs would report their best answers without knowing or caring about the origins of the inputs. For instance, once DNNs are trained with MNIST, they will always report one of the digits as the best answer even in response to alphabet letters. These indiscriminate answers to ‘out-of-training’ examples may result in critical errors under particular circumstances. Thus, DNNs need automatic systems to detect out-of-training examples to prevent catastrophic failures. We note that adversarially manipulated inputs can be considered

as out-of-training examples. Noting that CPL is reduced when adversarially manipulated inputs are introduced, we propose that the library networks and CPL can be used to determine if the inputs belong to the proper domains for inputs; when CPL values are too low, we should seek a second opinion (i.e., alternative DNN or humans’ opinions) or retrain the networks.

4.3 Future directions

In this study, we maintain the structure of the library networks and learning algorithms for functional connections as simple as possible. Instead of refining them, we focused on addressing the potential functional links between hidden layer activity patterns and DNNs’ decisions. In the future, we will extend the structure to handle more complicated tasks. More specifically, we will test the capability of the library networks which take a subset of hidden neurons (chosen sparsely and randomly). This ‘sparse’ sampling can reduce the dimension of the library networks, which may be necessary for a large-scale dataset or networks, and we will study the predictive powers of the sparse sampling library networks.

Table 1: We list the threshold (θ) values used to build library networks for the ResNet and calculate CPLs. Top rows show the ranges of θ tested for all 5 layers. The bottom rows show the θ chosen for calculating CPLs.

θ level	0	1	2	3	4	5	6	7
CN1	0.18	0.2	0.22	0.24	0.26	0.3	0.32	0.34
L1	0.64	0.66	0.68	0.7	0.72	0.74	0.76	0.78
L2	0.48	0.5	0.52	0.54	0.56	0.58	0.6	0.62
L3	0.5	0.52	0.54	0.56	0.58	0.6	0.62	0.64
FC	0.8	0.82	0.84	0.86	0.88	0.9	0.92	0.94
CNN	CN1	CN2	FC1	FC2				
Set1	0.55	0.75	0.75	0.8				
Set2	0.6	0.75	0.8	0.85				
Set3	0.55	0.65	0.65	0.65				
Set4	0.55	0.75	0.8	0.85				
Set5	0.6	0.7	0.75	0.75				
Set6	0.6	0.7	0.8	0.8				
Set7	0.6	0.7	0.85	0.85				
ResNet	CL1	CL2	CL3	FC				
Set1	0.72	0.58	0.62	0.94				
Set2	0.72	0.56	0.58	0.88				
Set3	0.74	0.58	0.6	0.9				
Set4	0.76	0.6	0.62	0.92				
Set5	0.78	0.62	0.64	0.94				
Set6	0.72	0.6	0.62	0.92				
Set7	0.72	0.62	0.64	0.94				

References

- [1] Amina Adadi and Mohammed Berrada. Peeking Inside the Black-Box: A Survey on Explainable Artificial Intelligence (XAI). *IEEE Access*, 6:52138–52160, 2018.
- [2] Guillaume Alain and Yoshua Bengio. Understanding intermediate layers using linear classifier probes. *arXiv*, 2016.
- [3] Shan Carter, Zan Armstrong, Ludwig Schubert, Ian Johnson, and Chris Olah. Activation atlas. *Distill*, 2019. <https://distill.pub/2019/activation-atlas>.
- [4] Gavin Weiguang Ding, Luyu Wang, and Xiaomeng Jin. AdverTorch v0.1: An adversarial robustness toolbox based on pytorch. *arXiv preprint arXiv:1902.07623*, 2019.
- [5] Dumitru Erhan, Yoshua Bengio, Aaron Courville, and Pascal Vincent. Visualizing higher-layer features of a deep network. Technical Report 1341, 2009.

- [6] Leilani H. Gilpin, David Bau, Ben Z. Yuan, Ayesha Bajwa, Michael Specter, and Lalana Kagal. Explaining explanations: An overview of interpretability of machine learning. *Proceedings - 2018 IEEE 5th International Conference on Data Science and Advanced Analytics, DSAA 2018*, pages 80–89, 2018.
- [7] Yerlan Idelbayev. pytorch resnet cifar10, 2018.
- [8] Alex Krizhevsky. Learning Multiple Layers of Features from Tiny Images. *Technical report, University of Toronto*, pages 1–60, 2009.
- [9] Yann Lecun, Yoshua Bengio, and Geoffrey Hinton. Deep learning. *Nature*, 521(7553):436–444, 2015.
- [10] Yann LeCun, Leon Bottou, Yoshua Bengio, and Patric Haffner. Gradient-Based Learning Applied to Document Recognition. *PROC. OF IEEE*, 1998.
- [11] Jung H. Lee. DynMat, a network that can learn after learning. *Neural Networks*, 116:88–100, 2018.
- [12] Jung Hoon Lee. hypothesis-building, 2019.
- [13] Zachary C. Lipton. The Mythos of Model Interpretability. In *ICML WHI*, 2016.
- [14] Xuan Liu, Xiaoguang Wang, and Stan Matwin. Interpretable Deep Convolutional Neural Networks via Meta-learning. *Proceedings of the International Joint Conference on Neural Networks*, 2018-July, 2018.
- [15] Aleksander Madry, Aleksandar Makelov, Ludwig Schmidt, Dimitris Tsipras, and Adrian Vladu. Towards Deep Learning Models Resistant to Adversarial Attacks. In *NeurIPS*, page 1706.06083, 2019.
- [16] Christoph Molnar. *Interpretable Machine Learning*. 2019.
- [17] Grégoire Montavon, Mikio L. Braun, and Klaus Robert Müller. Kernel analysis of deep networks. *Journal of Machine Learning Research*, 12:2563–2581, 2011.
- [18] Chris Olah, Alexander Mordvintsev, and Ludwig Schubert. Feature visualization. *Distill*, 2017. <https://distill.pub/2017/feature-visualization>.
- [19] Adam Paszke, Sam Gross, Soumith Chintala, Edward Chanan, Gregory Yang, Zachary DeVito, Alban Lin, Zeming Desmaison, Luca Antiga, and Adam Lerer. Automatic differentiation in PyTorch. In *NIPS Autodiff Workshop*, 2017.
- [20] Pytorch-team. Pytorch reinforcement examples, 2018.
- [21] Maithra Raghu, Justin Gilmer, Jason Yosinski, and Jascha Sohl-Dickstein. SVCCA: Singular vector canonical correlation analysis for deep learning dynamics and interpretability. *Advances in Neural Information Processing Systems*, 2017-Decem(Nips):6077–6086, 2017.
- [22] Cynthia Rudin. Please Stop Explaining Black Box Models for High Stakes Decisions. In *NIPS Workshop*, 2018.
- [23] Karen Simonyan, Andrea Vedaldi, and Andrew Zisserman. Deep Inside Convolutional Networks: Visualising Image Classification Models and Saliency Maps. *arXiv*, (1312.6034), 2013.
- [24] Wikipedia contributors. Receiver operating characteristic — Wikipedia, the free encyclopedia, 2019. [Online; accessed 28-September-2019].